PARIS VII
POLITECNICO DI TORINO

Master's Degree in "Quantum devices"

Master's Degree Thesis

Superparamagnetic iron oxide nanoparticles loaded in hybrid lipid/polymer nanoparticles as a multifunctional platform to treat cancer

Supervisors

Prof. Gianni CIOFANI

Prof. Carlo RICCIARDI

PhD Carlotta PUCCI

Candidate

Giulio AVVEDUTO

06 2020

Summary

Cancer is one of the main causes of death every year, according to Bray and Adams [1] more than 18 million cases were diagnosed in 2018 all over the world and these statistics are destined to increase of 40% within 20 years. Malignant tumours show an abnormal cells growth, which could potentially spread towards vital organs compromising essential functions and in the worst case, it could lead to the patient's death.
Some aggressive cancers may be difficult to treat because of the topology and drug resistance; for example brain tumours like glioblastoma multiforme (GBM) present complexity in being treated with conventional chemotherapeutic drugs because of the presence of the blood-brain barrier (BBB). Very few substances like carbohydrates and oxygen can go through it by the vascular system.
During the last years, nanomedicine showed promising results in the treatment of this kind of diseases. It is a quite new area of research investigating new ways of diagnosis, imaging and treatment by non-invasive methods. It combines medicine with nano-engineering in order to generate systems able to accomplish tasks otherwise difficult to achieve, such as accurate and targeted drug delivery and on demand therapy administration. It pledges incredible improvements with respect to older techniques for early diagnosis and high-resolution imaging.

Nanoparticles (NPs) are structures with all three physical dimension under few hundreds nm. Thanks to their size, surface/volume ratio and chemical composition they have peculiar and different properties. These can be tailor made and engineered quite easily in order to accomplish several tasks all at once. For example, high-resolution imaging can be achieved by attaching to the NPs' surface markers and fluorescent groups. Once the nanovector is internalized by target cells, by tracking the fluorescence it is possible to study the development of certain diseases with incredible accuracy.
Nanoparticles are also employed for drug delivery purposes, since they show a prolonged circulation half-life, reduced non-specific uptake, increased tumor accumulation through passive (enhanced permebility and retention (EPR)) or active targeting. Moreover, they are able to encapsulate a significant amount of drug

and deliver it in hostile environment. The delivery of conventional drugs can also be coupled with other therapies, like hyperthermia, to enhance the therapeutic efficiency.

Here hybrid lipid-polymer NPs (HLPNPs) arranged in a core-shell fashion combine the chemical stability of liposomes in aqueous environment with the high structural strength of polymers. Such systems in the last years have proven to be one of the best candidate for drug delivery [2, 3, 4].
The biodegradable polymeric core that encapsulates the drug is preferred to a lipidic one because of the higher structural strength, narrower size distribution and easy synthesis procedure, while the lipidic shell, usually coated with polyethylene glycol (PEG), provides biocompatibility in a biological environment, stealth effect towards the immune system (in particular the reticuloendothelial system) and steric stabilization.
The wide choice among raw materials and synthesis technique allows a great versatility for the best customization of the final product, so that it can result the most effective as possible. Several parameters define the quality of the delivery platform such as the amount of loaded drug, the targeting ability towards a selected site and potential secondary functionality. The most effective drug-delivery system should show maximum localization in the targeted area, long lifetime and controlled drug release profile.

The therapeutic efficacy of hyperthermia is well-known and since 1970s, controlled clinical trial demonstrated the efficacy of this technique against tumours. Induced and controlled heating has a double effect: it induces cells apoptosis and increases their sensitivity to chemotherapeutic drugs.
Apoptosis is the programmed death of the cell in response to a stress *stimulus*; the increase of heat between 41-47 °C is one of the stress initiator of the apoptotic pathway in tumour cells.
The physiological response to hyperthermia is to decrease the blood flux, which could lead to a shortage of oxygen and nutrients to the cell causing hypoxia; this effect is strongly enhanced in tumoural tissues since they have a disordered and sparse vascular architecture as compared to healthy tissues.
Moreover, recent studies showed how permeability of tumoural cells lysosomal membrane increases as a response to localized energy exchange; for instance, iron oxide NPs internalized in lysosomes, under alternate magnetic field (AMF) were able to induce lysosomal membrane permeabilization leading to the leakage of enzymes that triggered the initiation of the apoptotic pathway[5, 6, 7].
The biggest issue concerning hyperthermia is the difficulty to raise the temperature in a defined space inside a living body without compromising healthy tissues or without very invasive techniques. Recently a new technology called magnetic fluid

hyperthermia (MFH) has been developed. It consists of a colloidal suspension of magnetic nanoparticles (MNPs) that opportunely excited with an AMF is able to exchange heat with the immediate surroundings. The temperature rise is given by different physical effects, strongly dependent on the nature and the dimension of such MNPs. Superparamgnetic iron-oxide NPs (SPIONs) consist of a single (magnetic) domain iron-oxide NPs. Being highly biocompatible and tuneable in size and in shape SPIONs proved to be a versatile system to trigger hyperthermia and thanks to their typical dimension (few tens nanometer diameter) they could be embedded inside the aforementioned HLPNPs . The encapsulation facilitates the targeted delivery of MNPs dispersions. Furthermore, this also gives rise to a multifunctional platform able to deliver the medicine *in situ* by surface functionalization and, at the same time, to trigger the hyperthermic effect increasing the efficacy of the therapy.

HLPNPs loaded with both SPIONs and drugs are synthesized by self-assembly with different techniques. Among these, the emulsion/evaporation method and the nanoprecipitation stand out for their precision, efficiency and speed. Therefore, it would be of incredible interest to find one effective way of fabricating such particles loaded with both SPIONs and chemotherapeutics, in order to get a device able to administrate different therapies at the same time and test their efficacy against tumour cultures *in vitro*.

Table of Contents

List of Figures

Acronyms

AMF

alternating magnetic field

BBB

blood brain barrier

BHEM-Chol

N,N-bis (2-hydroxyethyl)- N-methyl-N-(2-cholesteryloxycarbonyl aminoethyl) ammonium bromide

cRGDfK

cyclo-[Arg-GlyAsp-D-Phe-Lys]

DMC

drug loadingdimethyl carbonate

DLPC

1,2-dilauroyl-sn-glycero-3-phosphocholine

DMAB

didodecyl dimethyl ammonium bromide

DMSO

diffusion limited coalescence

DNA

Deoxyribonucleic acid

DOPE

1,2-dioleoyl-sn-glycero-3-phosphoethanolamine

DSPE

1,2-Distearoyl-sn-glycero-3-phosphorylethanolamine

Dtxl

docetaxel

EM

electromagnetic

EMA

european medicines agency

EPC

ethylphosphocholine

EPR

enhanced permeability and retention

ESE

emulsion solvent evaporation

EtAt

ethyl acetate

FA

folic acid

FDA

food and drug administration

GBM

glioblastoma multiforme

GMS

glycerol monostearate

HLPNP

hybrid lipid/polymer nanoparticle

LMNV

lipid magnetic nanovector

MFH

magnetic fluid hyperthermia

MNP

magnetic nanoparticle

MRI

magnetic resonance imaging

NP

nanoparticle

PC

L-α-phosphatidylcholine (Soy,egg)

PEG

polyethylene glycol

PLGA

poly(lactic-co-glycolic acid)

PSD

particle size distribution

Ptxr-FLNP

folic acid decorated polymer lipid hybrid nanoparticles encapsulating cRGDfK modified paclitaxel

PY

production yield

PVA

polyvinyl alcohol

RBC

red blood cell

RES

reticuloendothelial system

RF

radiofrequency

siRNA

short interfering ribonucleic acid

SMF

static magnetic field

ScTNF

single chain tumor necrosis factor

ScFv

single chain variable fragments

SPION

superparamagnetic iron-oxide nanoparticles

TPGS

D-α-tocopheryl polyethylene glycol 100 succinate

TMZ

Temozolomide

THF

tetrahydrofuran

U-87 MG

Uppsala 87 Malignant Glioma

Chapter 1

Presentation of the dissertation

Cancerous cells exhibit an uncontrolled reproduction and a fast growth; for this reason, an early diagnosis and a punctual therapy improve significantly the chances of success of the therapy. Most of the chemotherapy drugs typically act against living cells, whether they are healthy or diseased and this poor recognition ability is one of the major drawbacks of chemotherapies.
This is just one among the many reasons why nanovectors could be of great help to fight against cancer: they could also safely deliver hydrophobic drugs to the target site, minimizing the dispersion in the surroundings and avoiding the rejection from the immune system.
Nanoparticles can be functionalized to enhance the interaction with tumoral cells while avoiding the healthy ones. The drug release profile can be also controlled by making nanocarriers *stimuli* responsive, in order to trigger the release with an internal signal like the change of pH in the cell environment or with external signals like electromagnetic pulses. Other *in vivo* properties, such circulating stability and longevity or diagnostic ability, can be tailored by *ad hoc* of modifications of the nanoparticles.
The aim of this dissertation is to present the latter improvements in nano-drug delivery and give the instruments needed to understand the basic principles behind this application. In particular, here we focus on the realization of hybrid lipid-polymer nanoparticles by two different procedure: emulsion/solvent evaporation and nanoprecipitation.
Here we also present a physical analysis on the hyperthermia produced by superparamagnetic nanoparticles in order to optimize the heating process for the best therapeutic effect.
Based on the theory exposed, a numerical simulation aimed optimizing some characteristic of loaded SPIONs to enhance the performances and the control on heating is presented.

Chapter 2

Nano-drug delivery

The need to find effective way to deliver drugs to the cancerous cells avoiding the interaction with healthy ones is a top priority for the oncological research. Basic requirements for these drug delivery systems are the biocompatibility and the stability in aqueous environment.
Nanostructures have the ability to stay in the blood circulatory system for a prolonged period and allow the release of hydrophobic drugs in hostile environment, with a controlled and tunable dose. Hence, they cause fewer plasma fluctuations with reduced adverse effects. Being nano-sized, these structures have a higher penetration potential inside biological tissues, facilitating the uptake of the drug by diseased cells and ensuring action at the targeted location. The uptake of nanoscopic systems by these cells is much higher than that of larger particles due to abnormalities in the vasculature of tumoral cells and the lacking of an effective lymphatic system. This peculiar accumulation of liposomes, nanostructures and macromolecular drugs around tumor tissues is known as EPR effect.
Another great advantage of these nanoparticles is the high surface/volume ratio, since various proteins can be attached to the surface enhancing the interaction with target cells with respect to healthy tissues, improving the efficiency and achieving a negligible level of side effects [8].

Polymeric nanoparticles have been widely used as they exhibit high structural integrity, stability during storage, and controlled release capabilities.

McCall and Sirianni [9] were able to produce poly(lactic-co-glycolic acid) (PLGA) based nanoparticles with an average size of (220 ± 70) nm for drug delivery application. PLGA is indeed a highly biocompatible copolymer, suited for biomedical application since it has been approved by the Food and Drug Administration (FDA) and the European Medicine Agency (EMA). It is quite versatile and shows good structural stability and low polydispersion for colloidal synthesis procedure.
Wang et al. [10] analysed several kind of NPs protocols like emulsion/solvent evaporation or nanoprecipitation, to fabricate PLGA NPs. PLGA showed indeed good solubility for both water miscible and immiscible solvents and great affinity with a wide variety of surfactant like D-α-tocopheryl polyethylene glycol 100 succinate (TPGS), polyvinyl alcohol (PVA) and didodecyl dimethyl ammonium bromide (DMAB). The batch realized with DMAB displayed smaller average dimension with respect to PVA, demonstrating that the reactants choice is crucial in order to finely tune the features of the product.
Feczkó et al. [11] reported improved drug loading for PLGA/PLGA-PEG (around 9% m/m) based nanocarriers with respect to liposomal ones ($\sim$4% m/m). This improved loading capacity is due to the hydrophobic behaviour of both drug and polymer, demonstrating the higher encapsulation potential with respect to lipid-based carriers.

Compared to polymeric nanoparticles, liposomes have long been considered as the ideal drug delivery vehicles since they show higher aqueous stability and biocompatibility being analogues of biological membranes.
Tapeinos et al. [12] synthesized a biomimetic nano-delivery system encapsulating temozolomide (TMZ) inside lipid based nanovectors. The choice of Glycerol monostearate (GMS) as primary lipid and Tween® 80 as stabilizer allowed small average dimension (below 100nm in diameter) and good cellular uptake by *in vitro* cultures: in fact, after 72 h of incubation almost 20% of U-87 MG cells volume was occupied by the nanovectors. Lipid-based systems can be easily disposed by RES showing no toxic effect, but for the same reason their bio availability is strongly limited. Moreover, liposomes present some drawbacks, suche as the lack of structural integrity resulting in drug leakage and instability during storage.

2.1 Hybrid lipid/polymer nanoparticles

In order to combine the advantages of both polymers and lipids, hybrid system arranged in a core-shell fashion have been realized. Hybrid Lipid-Polymer nanoparticles could be a very powerful tool for the fight against cancer. The selection of an optimal delivery vector is fundamental to ensure an efficient delivery, stability and minimize toxicity risks.

The polymeric core ensures structural stability to the drug carrier over time and guarantees a good encapsulation of the drug inside the matrix. The lipidic shell coating offers steadiness inside an aqueous environment because of the amphiphilic behaviour of phospholipids: inside an aqueous solution, indeed, they tend to self-assemble in closed structure, guided by electrostatic interactions of the hydrophobic tail and hydrophilic head. The lipid shell also protects the inner core from possible infiltration, degradation and load leakage, enhancing the lifetime of the carrier.

Figure 2.1: block composition of HLPNPs loaded with both drugs and SPIONs

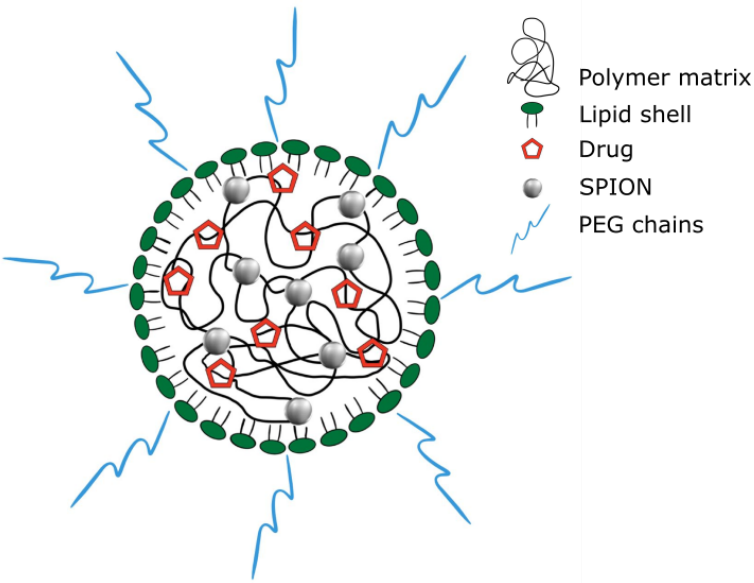

Similar to the pegylation of polymeric nanoparticles to enhance the bioavailability, lipid–polyethylene glycol (PEG) is often used in lipid NPs formulations to prolong the in vivo circulation time; moreover, modifying the end group of the PEG chains with methoxyl groups has been shown to lower the response of the immune system toward HLPNPs , resulting in lower immunogenicity and enhanced retention in the biological environment[3, 13].
Besides the enhanced stealth effect, the PEG coating ensures steric stability, avoiding undesired aggregation of NPs in order to prolong circulation half-life up to 50 h [14].
Zhang et al. [15] demonstrated how PEG chains avoided the coalescence of particles providing a long lasting colloidal steadiness.
In another study conducted by Hu et al. [16] to further improve stealth effect and overcome PEG related immunological response, polymeric nanoparticles were coated with red blood cells (RBC)

membranes. They thus compared half-life circulation time and retention of both PEG and RBC-membrane coated nanoparticles: RBC-membrane coated NPs showed a half-life time about 150% higher with respect to the PEG- coated ones, exhibiting also superior retention after 24 h incubation ($\sim$ 29% vs $\sim$ 11%). Optimization of core and shell composition can result in tunable drug release profile. Furthermore, drugs can be adsorbed on surface or encapsulated in the core thanks to the amphiphilic behaviour of the shell; therefore, both hydrophilic and hydrophobic drugs can be transported, even at the same time, enhancing the efficiency of this class of nanovector [17, 18].

2.2 Fabrication procedure

There is a wide range of techniques to synthesize hybrid lipid-polymer nanoparticles. Less common used techniques involve spray drying [19] or soft lithography particle molding [20] but most common procedures involves one or two step methods since they are faster, cheaper and they are able to meet all requirements for a given application. Here, we focus on emulsion/solvent evaporation and nanoprecipitation methods. Even if they seem similar from a practical point of view, they rely on completely different principles.

2.2.1 Emulsion/solvent evaporation

Figure 2.2: ESE schematic procedure. Image provided by Wang et al. [10]

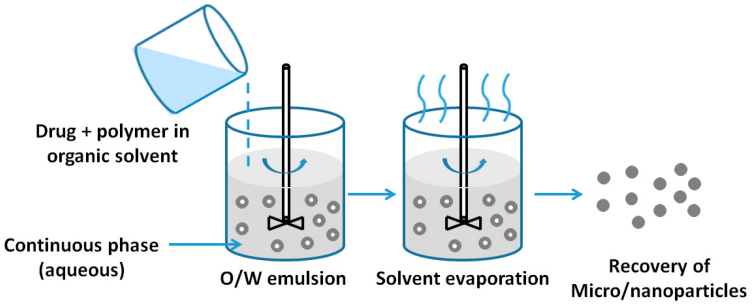

In the emulsion/solvent evaporation, the polymer together with the hydrophobic drug are dissolved in an organic solvent immiscible in water. Once the solution is homogenized, it is then poured dropwise into a water phase containing the surfactant (or the phospholipids in the case of HLPNPs). By means of a magnetic stirrer or a sonicator the mixture is emulsified in small, micro and nano droplets of oil (with all its solutes) suspended in the water phase [21].
Due to its amphiphilic nature, the surfactant (or the phospholipids) tends to deposit at water/oil (w/o) interface. The formation of NPs is driven by self-assembly and no molds are used. The organic solvent is then evaporated by magnetic stirring in a thermostated bath or in a rotatory evaporator under reduced pressure. The polymeric core hardens as soon as the organic solvent is removed: the result is a colloidal dispersion of HLPNPs in water [22]. Such solution is usually centrifuged and rinsed to filter out all the unreacted species.
The selection of the surfactant is thus crucial to determine also physical properties of the final nanoparticles. For example Hariharan et al. [23] reported that when cationic surfactants like DMAB were employed, the average particle dimension resulted smaller as compared to when realized with non-ionic surfactants like polyvinyl alcohol (PVA).

Colloidal stability is another critical property that these kind of systems must possess. Electrostatic stability is achieved when the electrostatic interaction between the partially charged NPs surface wins over their tendency to coalesce or aggregate. Indeed polymeric NPs show a predominant hydrophobic behaviour, thus they tend to aggregate, decreasing the surface/volume ratio. This phenomenon results in aggregation of small NPs in larger ones, in order to minimize

the surface exposed to water.
In order to determine the stability of such systems, ζ-potential of the particles is measured. Normally one defines a colloidal suspension stable when $|\zeta| > 30$ mV.
The right choice among different surfactants to cover the NPs is critical [24]; nonetheless nanovectors realized with PVA and TPGS by Win and Feng [25] reported a similar average size ($\sim$ 260nm / $\sim$290nm), PVA NPs had a ζ-potential of $\sim$-18 mV vs $\sim$-30 mV for TPGS ones.

The concentration of the reactants also plays a main role for the final size, drug loading and encapsulation efficiency of the nanoparticles. Cheow and Hadinoto [26] synthesized soy PC/PLGA hybrid NPs through ESE method and found that when the lipid/polymer (L/P) ratio was below 15%(w/w) the average size was roughly 800-1000 nm due to particle aggregation. By increasing the L/P ratio above 15%, the NPs size was reduced to $\sim$260 nm; the optimal L/P ratio was found to be at $\sim$30%, for which the production yield reached a maximum ($\sim$ 80%). Production yield (PY) is defined as the mass of nanoparticles recovered divided by the sum of the mass of reactants; therefore a PY of 100% would imply that the totality of reactants has been processed to form NPs and nothing was wasted during the synthesis procedure. In the same way, Liu et al. [27] found that for 1,2-dilauroyl-sn-glycero-3-phosphocholine (DLPC)/PLGA NPs higher L/P concentration resulted in smaller average particulate size: by varying DLPC concentration from 0.1% to 0.01% (w/v) the particle size increased from $\sim$240 nm to $\sim$435 nm reducing also the encapsulation efficiency from $\sim$42% to $\sim$15%.
The encapsulation efficiency is defined as the ratio between the incorporated drugs weight with respect to the original weight used for the initial formulation. This property strongly relies on the hydrophobic interaction between the polymeric core and the loaded drug and on the dimension of the nanoparticles as well. Zhang et al. [15] reported that for higher L/P ratios DSPE-PEG/PLGA NPs loaded with docetaxel (Dtxl) showed a reduced size, leading to a consequent reduced encapsulation potential; at the same time the small size increased the surface pressure reducing the drug leakage and thus enhancing encapsulation efficiency.
In this regard, an interesting observation is reported by Chu et al. [28] that showed how to synthesize HLPNPs (PEG-PE/PLGA) with a diameter below 50 nm by increasing the L/P up to 300%; despite the reduced dimension they measured an encapsulation efficiency of about $\sim$60% for Doxorubicin. In addition, Wang et al. [10] also pointed out how the selection of organic solvent can influence the final size of the product; for example they found that ethyl acetate (EtAt) produced smaller and more uniformed size nanoparticles than dimethyl carbonate (DMC) since the first is more water miscible. Lastly, a great advantage this synthesis method guarantees is the possibility to encapsulate hydrophilic drugs inside the nanovector by performing a double emulsion.
The operative way is similar [29]: at first small droplets containing the hydrophilic molecule are emulsified in an organic solvent containing polymer and an emulsifying agent, ethylphosphocholine (EPC) in the case mentioned. Due to the amphiphilic nature of EPC the reaction lead to inverse micelle self-assembly. Then the procedure follows identically the ESE method described before.
This method allows generating HLPNPs with a hollow core containing a water solution of hydrophilic molecules like short interfering RNA (siRNA) and at the same time allows the co-delivery of hydrophobic drugs encapsulated in the polymeric matrix [17].

2.2.2 Nanoprecipitation

Nanoprecipitation, firstly proposed by Fessi et al. [30], is a one-step technique, faster and cheaper than ESE; the setup is quite similar with few, but crucial, differences.

Contrary to ESE, the polymer and the drug are dissolved in a water miscible solvent (e.g. acetone, THF, DMSO). Then the solution is dropped into a water phase, so that the organic solvent start to diffuse and the saturation of the polymer goes beyond the limit, due to its insolubility,as the water fraction increases.

Nanoprecipitation can be divided in 3 steps [31]: nucleation, growth and aggregation. The first step correspond to the formation of the first nuclei of the NPs and it is triggered when the limit of solubility of the polymer in the mixture organic solvent/water is passed. Then the polymer starts to self-assemble in small aggregates, forming a polymeric array and at the same time encapsulating the drug. Once the loaded core is formed, the unbound polymeric chains start adding to the already formed structure in a spontaneous process and no additives are required to favour the growth. However, to avoid coalescence it is important to keep the stirring while the dissolved surfactant in the aqueous phase covers the polymeric cores.

Figure 2.3: schematic representation of Nanoprecipitation. Image provided by Wang et al. [10]

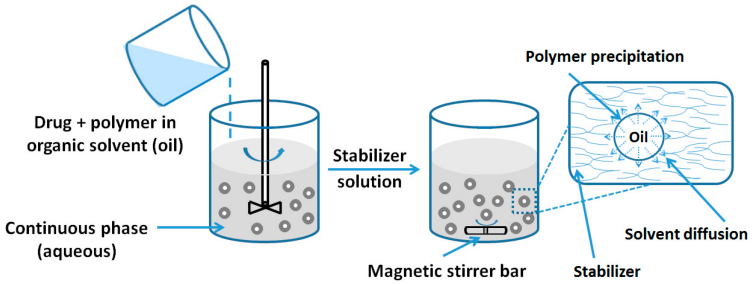

Nucleation happens in few milliseconds, therefore finely dosing the concentrations of every component is a key step [24]. Lebouille et al. [32] investigated a mathematical model in order to determine the size of produced HLPNPs . Depending on the conditions of synthesis like the initial L/P, the molecular weight of reactants and the mixing time, it is possible to approximate the growth of the nanoparticles through the "Diffusion limited coalescence" or the "slow mixing" limits. In the DLC limit, the final size is purely determined by a set of fluid dynamics equations, and the final radius depends linearly on the concentration of the surfactant. Indeed, the surfactant hinders the coalescence of small nanoparticles.
In slow mixing limit the probability for two particles to meet falls drastically, so that the final radius of the synthesized nanoparticles grows as $R_{final} \sim (c_{p0}\tau_{mix})^{1/3}$ where τ_{mix} is the mixing time and c_{p0} is the concentration of polymer nanoparticles developed right after the mixing.
Zhang et al. [15] and Chan et al. [33] found that a L/P ratio about $\approx$ 15% was optimal to cover the polymeric core for PLGA-lecithin/DSPE-PEG HLPNPs of about $\approx$60 nm-80 nm, while Yang et al. [34] found that to realize 65 nm HLPNPs, the L/P ratio needed was $\sim$10% using a mPEG-PLA core and N,N-bis (2-hydroxyethyl)- N-methyl-N-(2-cholesteryloxycarbonyl aminoethyl) ammonium bromide (BHEM-Chol) as the lipid shell.
Nanoprecipitation shows very good results concerning the quality of the synthesized product, giving rise to objects with narrow particle size distribution (PSD) and high degree of tunability; for these reasons during the last years more and more research groups focused on improving this method.
In order to achieve a fast and homogeneous mixing, Fang et al. [21] employed a bath sonicator for 5 minutes (42 kHz, 100 W), increasing the production rate about 20 times when compared to standard mixing procedure. In this way, they also eliminated the solvent evaporation step, by using a small amount of organic solvent, which quickly evaporated during the self-assembly process. PLGA-lecithin/DSPE-PEG HLPNPs average size was about 65nm showing minimum dispersion, and stability tests demonstrated good stability for almost a week.
To further reduce the dimension of HLPNPs, a modified procedure called 'Flash nanoprecipitation' could be employed. It consists in the mixing of the aqueous-lipid solution with the

polymer (and drug) dissolved in an organic solvent through a static mixer comprising a Tesla structure along a microfluidic channel. This setup ensures a fine control over the L/P and a considerable reduction of the nucleation time.

Using this configuration, Valencia et al. [35] observed that the dissolution of the organic phase occurred much faster with respect to the standard procedure, leading to the formation of more homogeneous polymeric cores. In this way, they were able to control the NPs size from ∼35 nm to ∼180 nm by tuning the viscosity and the polymer concentration of the mixing solution, noticing also that the lipid concentration did not have a significant influence on the final size, but it prevented the aggregation of already formed polymeric cores. The molecular weight also have an impact on the final size of the nanoparticles[15, 33].
Lately, Kim et al. [36] investigated how the Reynolds number (Re) of the flow in the channel could influence the throughput rate, demonstrating that for Re$\geq$ 75 production rate could be enhanced by almost 1000 times with respect to conventional methods.
Re is an dimensionless number that in fluid dynamics usually indicates the regime of the flow in a channel. For low Re the flow is laminar, hence two fluids flowing in the same channel do not mix. The higher is the Re the more turbulent becomes the flow. These research groups showed that the turbulence along the channel favoured the mixing between the two solutions, so that the interaction rate between reacting species increased and the water miscible organic solvent dispersed more quickly, enhancing the control over the size distribution of the throughput.
This set-up brought several improvements to the quality of the product, lowering the average size and raising the throughput. Besides the biocompatibility, the safety for the user and the therapeutic effectiveness, the basis behind clinical translation and application stand on mass scale production and high quality reproducibility, thus all these advancements represent how much this field is growing and soon clinical application could be investigated [37, 38].

2.3 Improvements

Nanoprecipitation and ESE methods give quite different results. In terms of size, NPs prepared by nanoprecipitation usually present smaller size down to 20-40 nm [3], with a very low polydispersity index down to 0.08 [21], while ESE products are usually characterized by a broader size distribution along with larger average size [10, 15, 17, 21, 23, 24, 25, 26, 27, 28, 29]. Even though nanoprecipitation usually gives better results, other preparation procedures can be followed according to specific requirements. For instance, if the polymer is not soluble in water-miscible solvent, then the nanoprecipitation technique cannot be used. Moreover, parameters like the encapsulation efficiency or drug loading depend not only on the fabrication procedure, but also on intrinsic properties of the vector and the drug.

The nature of every component strongly influences the characteristic of the synthesized HLPNPs [3]. For instance Zheng et al. [39] reported that to prepare ≥150 nm PLGA core and egg PC/DOPE shell HLPNPs they required a L/P ∼430%, while Yang et al. [34] showed that a L/P ∼10% was sufficient to prepare 65 nm HLPNPs when used pegylated DSPE as lipid. Both lipid species are non-ionic and have similar molecular weight, thus for higher L/P one expected smaller nanoparticles; however, in this case it is the opposite, confirming the fact that every species behave differently and produces different result, sometimes hardly predictable.

Composition, size and functionalization of these delivery platforms have an impact also on the interaction with cells. Therefore, the behaviour of HLPNPs toward *in vitro* cultures must be carefully studied and the efficiency in their therapeutic action needs to be tested also on *in*

vitro models before applications.
Zhang et al. [15] compared several aspect of non-hybrid and hybrid PLGA based NPs: beside the higher colloidal stability of the hybrid-counterparts, interestingly HLPNPs also show a more efficient drug encapsulation (∼60% versus ∼40% obtained for non-hybrid polymeric NPs). On the other hand, hybrid PLGA-based NPs show a slower release profile with 90% of the drug released after 120 h, while PLGA NPs reached this value after 70 h. This difference relies mainly on two factors: the interaction between the loaded drug and polymeric core and the presence of the lipidic shell.
As already said, the interactions between loaded drug and polymeric core plays a major role in the encapsulation efficiency and release dynamics of such vectors: high hydrophobic molecules show strong binding with the hosting matrix, enhancing the loading capacity but at the same time hindering the release.
On the other hand, a lipid layer dividing the core from the aqueous environment avoids the drug leakage due to the degradation of the structure.

The necessity to further improve the release profile and enhance the efficacy of the drug-loaded nanovector could be satisfied by a local increase of temperature inside the nanovector environment. Magnetic nanoparticles hyperthermia thus could be a smart way to go beyond these issues.

Chapter 3

Hyperthermia generation

Hyperthermia is a therapy that exploits therapeutic effects for tissues exposed to temperature around 41-47°C. It was found that tumor cells, if heated, underwent to apoptosis usually causing minimal damage to healthy cells [40, 41]. The cancer and healthy cells have a different response to the increase of temperature, with tumor cells being more sensitive than healthy ones. For these reasons hyperthermia can be combined with chemotherapies in multimodality treatment, providing a better result: the combination of the two could enhance the cytotoxic effect of drugs against tumoral cells [42, 43] and at the same time increase the local blood flow enhancing the drug supply to the targeted site overcoming multidrug resistance.

3.1 Localized Hyperthermia

Hyperthermia can be generated through different methods [44]. The most common are infrared or microwave radiation, ultrasound stimulation or even probe heating implanted by surgery. However, these techniques can produce unwanted hot spots in proximity of the target area causing side effects [45]. Electromagnetic (EM) induced heating has low penetration depth and it is hard to accurately heat small spots or deep-seated tumors without using any implanted device; for this reason, magnetic fluid hyperthermia (MFH) represents a big step forward for hyperthermia treatments and it may definitely overcome these issues.
It consist in the injection of a colloidal suspension of MNPs in the site of interest and then in triggering the generation of heat by applying an AMF. These magnetosensitive colloidal suspensions could be driven and confined in very narrow spots and they could be able to reach deep-seated tumors. Distribution of such NPs in the cancerous area strongly influences the heat dose administered during the treatment. Wang [46] found that localized NPs generated a more effective anti-tumor effect for low power heating. Moreover, by using low power AMF, such treatments would result safer for the patients, avoiding possible side effects.

3.2 Magnetic requirements for bio-application

The magnetic properties of materials arise from the spin and orbital motions of the electrons in the atoms. Such spin-orbit electron motion can produce a net magnetic dipole moment since, for the Ampère-Laplace's law, a charge flowing around a closed path generates a net magnetic moment [47].

In some materials, defined paramagnetic and diamagnetic materials, the interaction between magnetic moments is zero, whereas ferromagnets and antiferromagnets show a negative or positive (respectively) energy contribution due to exchange interaction between neighbouring magnetic moments, resulting in parallel or antiparallel spin alignment.
To distinguish between the different types of magnetic materials, their response to an external magnetic field is investigated. The most commonly used magnetic material for biomedical applications are ferromagnetic, ferrimagnetic and paramagnetic, since they results the most effective, reliable and controllable.
In ferromagnetic materials there is a spontaneous alignment of the atomic magnetic moments parallel with their neighbours below a critical temperature, called the Curie temperature. Below T_C, since the neighbouring interaction is strong enough to overcome a possible thermal inversion of the magnetic moment, a ferromagnet can have a net magnetic moment in zero applied magnetic field fig 3.3. However, under the influence of an applied magnetic field, the atomic magnetic moments will align parallel to the applied magnetic field. Above T_C the material acts as a paramagnet.
Ferrimagnets are a special class of antiferromagnets, where the antiparallel atomic moments have different magnitudes. This means that ferrimagnets can exhibit a non-zero net magnetic moment at zero applied magnetic field, but smaller than ferromagnets .
In contrast to diamagnetic materials that have all electrons paired, paramagnetic materials have unpaired electrons. They hence display a positive magnetic moment response to a positive applied magnetic field in addition to the diamagnetic negative response from their paired electrons. This paramagnetic response overcomes the diamagnetic one, but the individual atomic magnetic moments do not have any exchange interaction, so magnetic moments point in all directions, resulting in zero net moment in zero applied magnetic field.

Figure 3.1: magnetic moments disposition for ferromagnetic, antiferromagnetic, ferrimagnetic and paramagnetic materials

There is a wide variety of MNPs and, according to their chemical composition, shape and size they behave differently [48, 49, 50, 51, 52]; as one can imagine when comes to biomedical application just few MNPs respect all constraints related to the case.
Here, we focused on superparamagnetic iron-oxide NPs (SPIONs) for several reasons: besides their magnetic properties, they have already been approved by FDA and EMA for biomedical applications and they show excellent biocompatibility. Furthermore, they can be easily synthesized in laboratory by procedures already optimized [2, 53, 54]. Usually a mixture of $FeCl_3 \cdot 6H_2O$ and $FeCl_2 \cdot 4H_2O$ react in a solution with ammonium hydroxide at high temperatures ($\sim$80 °C) for one and a half hours after the addition oleic acid. The latter is used as capping agent, hindering the further growth of the particulate and ensuring a high degree of monodispersion: in the case reported, a high monodisperse population of 10 nm SPIONs was synthesized.

Iron-oxide exists in several allotropic forms like magnetite (Fe_3O_4) and maghemite (γ-Fe_2O_3), according to the ratio between Fe^{3+} and Fe^{2+}. Macroscopic crystals show ferrimagnetic and ferromagnetic behaviour below the T_C (858 K and 958 K for the two allotropes), but under a certain dimension, they behave as paramagnets, even at room temperature. This phenomenon is called superparamagnetism and it occurs when the size of the crystal falls below a certain

limit called critical diameter. Below a certain volume it is energetically favourable to form a single domain crystal instead of having several domain walls [50, 55]. This dimension is strongly dependent on several properties like the anisotropy energy or the saturation field; however, Iron-oxide based NPs under normal condition (pressure, T, stress...) exploit superparamagnetic effects below few tens nm of diameter. All superparamagnetic materials are single domain, but not every single domain crystal is superparamagnetic [47, 48]: according to the shape, the temperature, the stress (etc...), some single domain systems can exploit non zero coercive field fig 3.2.

Figure 3.2: superparamagnetic transition for small dimension single domain nanoparticles.

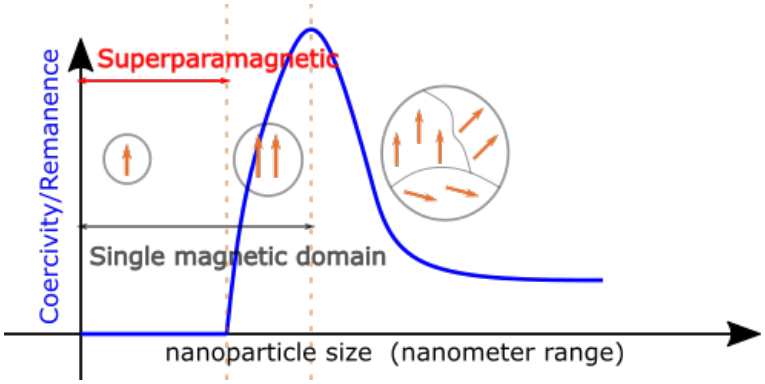

Being superparamagnetic crystals, the system show zero coercive field and high saturation field even at room temperature, allowing superparamagnetic heating for clinical application. Induced currents (usually called eddy currents) do not play any relevant role in this context because of the reduced size of such MNPs and because of the very low resistivity (hence Joule effect is always considered negligible) [56, 57]. In order to build a model able to describe the heating process of such systems, one usually refers to the hysteresis curve that describes how the crystal magnetization responds to an applied external magnetic field [56, 58, 59].

In particular, in this approximation, the heating is due to intrinsic losses that can be measured by evaluating the area of hysteresis cycle here represented by the shaded area.

Figure 3.3: hysteresis curves for ferromagnetic, paramagnetic and superparamagnetic materials

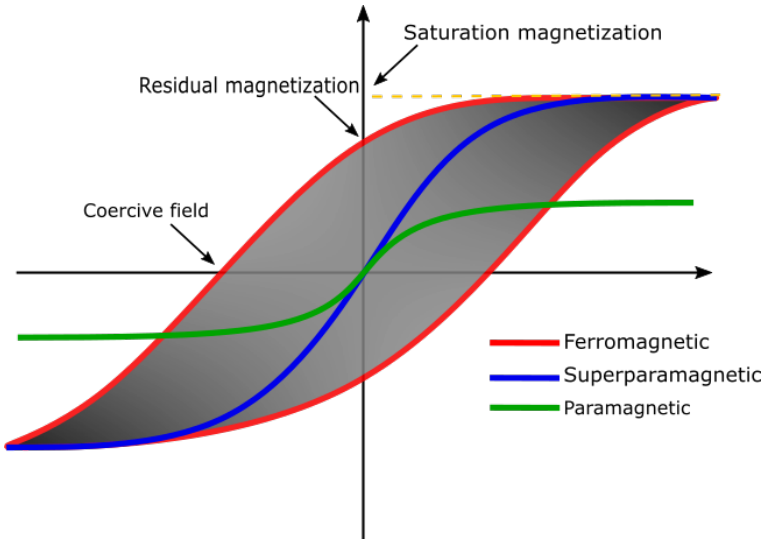

AC field is able to saturate magnetization in both orientation for each period, thus for each cycle the energy dissipated is [47]

$$W_{heat} = -\mu_0 \oint \vec{M} \cdot d\vec{H} \qquad (3.1)$$

For superparamagnetic crystals such hysteresis loop is extremely narrow with a null area, having by definition zero coercivity then zero remaining magnetization [51, 58, 60].

However, they possess a large saturation magnetization at room T, larger than those of paramagnetic materials, hence the definition "superparamagnetic".
A critical feature that makes this class of single-domain system suitable for hyperthermia is the characteristic timescale, strongly dependent on the dimension of the system. Such kind of response fig 3.3 is referred to static or slowly varying external field, for which the oscillation

frequency f is lower that the characteristic reversal time [47, 57].

To an applied magnetic field

$$H(t) = H_0 cos(\omega t) = Re[H_0 e^{i\omega t}] \tag{3.2}$$

corresponds a magnetization

$$M(t) = Re[\chi H_0 e^{i\omega t}] \tag{3.3}$$

with $\chi \in \mathbb{C}$ being the magnetic susceptibility. There is one term composing $M(t)$ which phase is shifted of a quarter period $H(t)$ and therefore linked to the losses, as can be easily seen by substituting (3.3),(3.2) in (3.1)

$$W_{heat} = -\mu_0 \int_0^{2\pi} H_0[\chi' cos(\omega t) + \chi'' sin(\omega t)] dH_0 cos(\omega t) = \mu_0 \pi H_0^2 \chi'' \tag{3.4}$$

that correspond to the energy acquired by the surroundings of the particle for each oscillation of the external field.
Trivially, the associated heating power is given by

$$P = W_{heat} f \tag{3.5}$$

where $f = \dfrac{\omega}{2\pi}$ is the AC field frequency.

The treatment is analogous to the Debye's theory for dipole electric susceptibility [56, 57, 63, 64]

$$\chi'' = \frac{\omega\tau}{1 + (\omega\tau)^2} \chi_0 \tag{3.6}$$

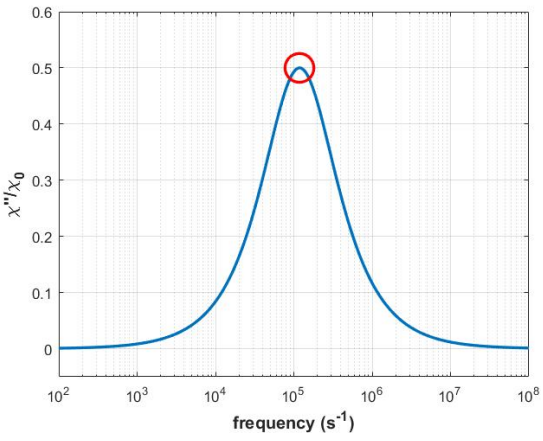

Figure 3.4: χ'' as a function of frequency. For f ∼100kHz shows a peak, corresponding to a maximum for (3.4). Even though (3.5) is a monotone increasing function of f it has to be maximized within physiological limits [49, 61, 62]

From this equation it becomes more clear why the time scale has to be taken into account for the study of such kind of systems: for low frequency the relaxation time is extremely short when compared to the oscillation time, therefore it seems like if the particle feels the average effect of several relaxation processes that lead to a zero net magnetic moment, hence no energy dissipation.
When the frequency increases, the timescale of the relaxation process and the oscillation are comparable and χ'' has a peak when $\omega\tau = 1$; therefore, the heating by relaxation is maximized at quite high frequencies.

In order to determine the frequency range more suitable for this kind of applications, one focuses on the relaxation process that determines τ in (3.6), which is defined by two concurrent events called Néel and Brownian relaxation processes.

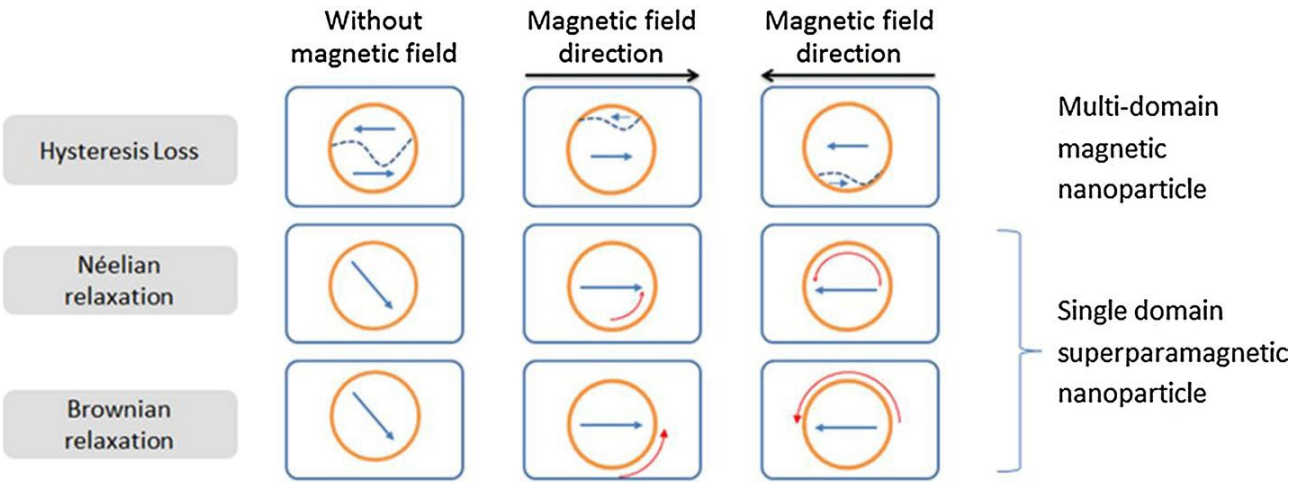

Figure 3.5: Different heat generation models in a magnetic nanoparticle in response to the alternative magnetic field. The short straight arrows represent the magnetic moment direction, the curved arrows represent the movement or change in direction, and the dash lines represent the domain boundaries in multi-domain particles. Image provided by Suriyanto et al. [62]

3.3 Néel-Brown relaxation processes

Typically MNPs magnetic properties are strongly dependent on crystalline orientation [50, 55], especially for single domain structures. Iron-oxide magnetocrystalline anisotropy leads to the preferntial alignment of the magnetic moments along the so called "easy axis" in order to minimize the energy of the system. It represent the direction in the crystalline structure for which the magnetization alignment to an external field requires minimum energy.
This energy contribution coming from anisotropy reads [55, 64]

$$E_{anis} = KV sin^2\theta \tag{3.7}$$

Figure 3.6: representation of the barrier potential along θ with the two minima for the two angles minimizing (3.7).

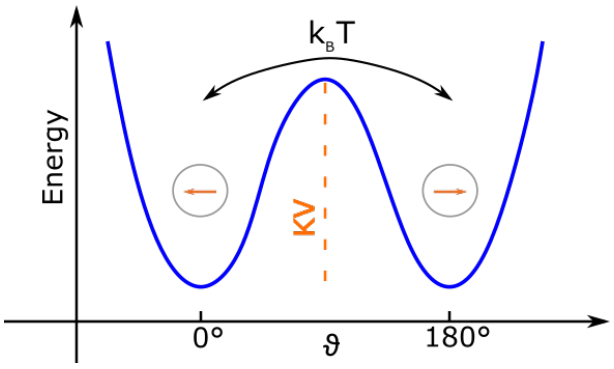

where θ is the angle between the magnetization of the MNP and its easy axis, K is the magnetic anisotropy density and V is the magnetic Volume (fig 3.6).
Assuming an initial magnetization M_i, the rate of decrease at any time follows the Arrhenius law [65]:

$$M = M_i e^{-\frac{E_{anis}}{k_B T}} \rightarrow -\frac{dM}{dt} = \frac{M_i}{\tau_0} e^{-\frac{E_{anis}}{k_B T}} \tag{3.8}$$

τ_0 is a semi-empirical constant usually referred as attempt frequency ($\sim 10^9 Hz$) [55, 59, 47, 64]. Trivially one obtains

$$\frac{1}{\tau_N} = \frac{1}{\tau_0} e^{-\frac{E_{anis}}{k_B T}} \tag{3.9}$$

The Brown relaxation process comes from the physical rotation of the particle inside a viscous environment and can be evaluated through the Brownian relaxation time[56, 57, 58, 60, 62, 64]:

$$\tau_B = \frac{4\pi\eta r_h^3}{k_B T} \tag{3.10}$$

The friction between the surface of the NPs and the environment generates heat.
These two relaxation processes can be seen as competitive, hence the total relaxation time is defined as $\tau_{tot}^{-1} = \tau_N^{-1} + \tau_B^{-1}$.

Usually for colloidal suspensions of MNPs, the energy balance equation involves also other terms correlated to dipolar, van der Waals and steric interaction. It has to be noted that, in the case under analysis, this system is not that simple. When the SPIONs are well dispersed in the viscous core of an organic nanoparticle, like in the case of HLPNPs, the interaction between iron-oxide NPs can be neglected [64, 66].

3.4 Numerical optimization

In the attempt to optimize the dimension of SPIONs loaded in HLPNPs in order to obtain the most efficient heat generation and in a multiplatform delivery vector some numerical simulations are performed here.
The first thing to keep in mind when working for medical and biological applications is that there are constraints correlated to the biocompatibility and safety of the system and the kind of treatment. In the particular case treated here, for example, frequency and amplitude of the applied magnetic field need to be carefully selected and should not exceed some established limits [49, 61, 62].

Figure 3.7: relaxation time (τ) dependence with respect to the size of the single SPION

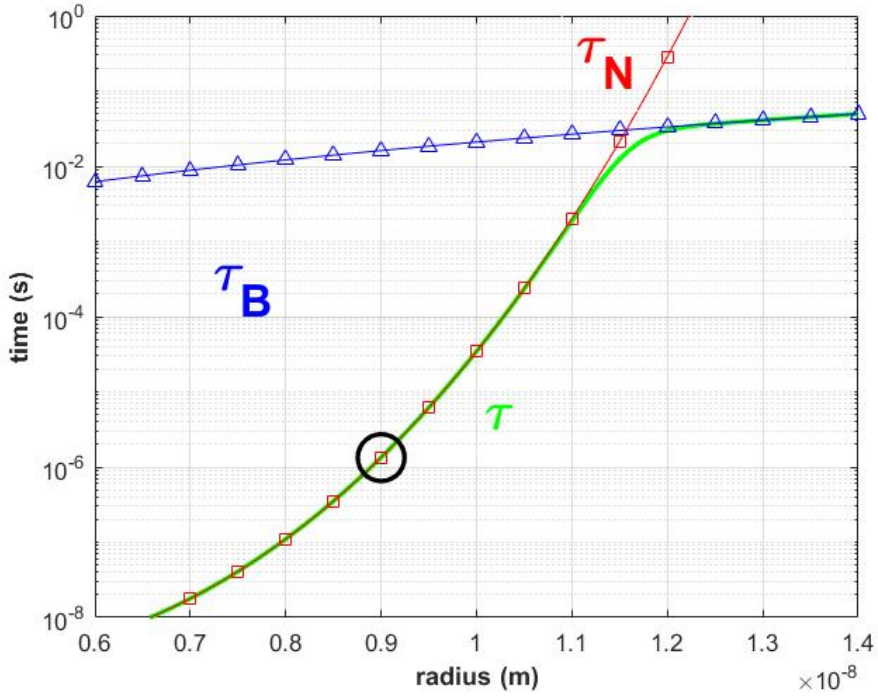

It is considered safe a threshold of $f \cdot H < 4.85 \times 10^8$ $\mathrm{Am^{-1}s^{-1}}$, but usually MFH is investigated with fields around hundreds of kHz [47, 60].
Here, a system composed by a viscous environment made by PLGA polymer, with a viscosity η=4 kg $\mathrm{m^{-1}s^{-1}}$ loaded with SPIONs was analysed[57, 67]. Iron oxide anisotropy (bulk) constant settled was $K_{anis} = 1.3 \times 10^4 \mathrm{J\ m^{-3}}$ [68].

Maximizing the losses (3.6) at 100 kHz, one gets that the optimal SPIONs size should be around 9 nm. Furthermore, it is evident from fig 3.7 that the Néel relaxation process dominates above Brown's relaxation, making this heat exchange less sensitive to surrounding fluctuation.

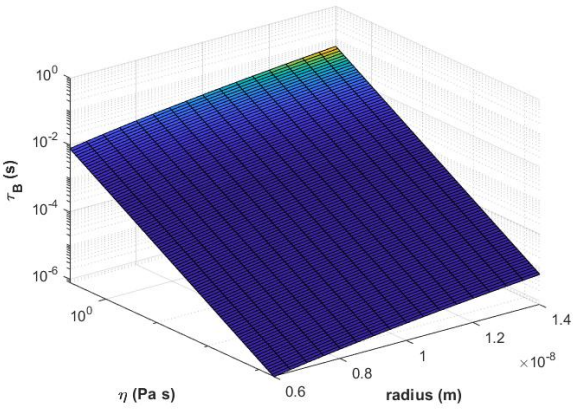

Figure 3.8: evolution of τ_B with respect to the size of the SPION and the medium viscosity

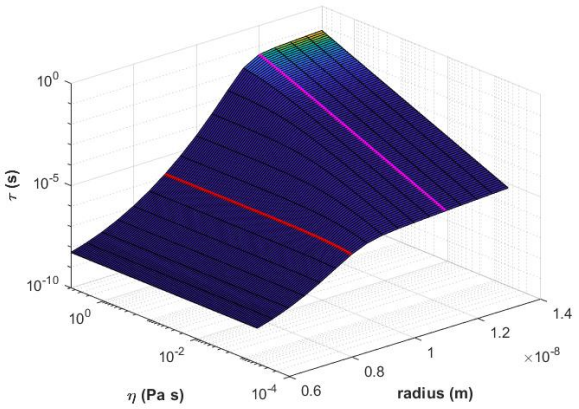

Figure 3.9: variation of τ with respect to the size of the SPION and the medium viscosity

PLGA, in particular, has a glass transition close to hyperthermic working temperature, meaning that during AMF stimulation the polymeric matrix could go through a phase transition changing substantially its viscosity.
As we can see from the red line, fig 3.9 the relaxation time remains still even for high fluctuations of η when the SPIONs radius stays below 10 nm. However, for larger size, τ_B could become the dominant process making τ sensible to the surrounding viscosity changes fig 3.8.

Therefore, by tuning properly the properties of such MNPs it is possible to control the heat exchange in order to exploit the glass transition of the loading matrix and to ease the release of the load under an external *stimulus*.

Lastly it was evaluated the dependence of SAR with respect to the SPIONs size fluctuation. Typically, to express heating effects for biomedical application a physical quantity that is the Power per unit of weight, usually referred as specific absorption rate (SAR) or specific loss rate (SLR) according to the convention, is used.
Besides the other approximation limits, a slow varying field approximation was considered: the amplitude of the AMF is constant over the NP volume being $\lambda = \dfrac{c}{n_x f} \sim \dfrac{10^3}{n_x}\text{m} \ggg$ hundreds nm. Under this assumption one can consider $P = SAR \times V \times \rho$, hence from (3.4),(3.5) and (3.6) one gets fig 3.10.
From fig 3.10 it is evident that in order to achieve therapeutic level of SAR, the size of the loaded SPIONs has to be highly monodisperse.

Figure 3.10: SAR dependence on SPION size

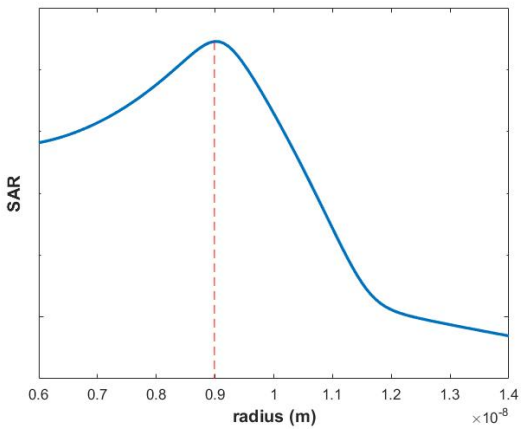

Chapter 4

Stimuli responsive multifunctional drug delivery systems

Advancements in the field of nanotechnology for cancer treatment with nanoscopic devices led to the development of multitask platforms able to accomplish different assignments all at once. Here, by combining superparamagnetic nanoparticles capacity to induce magnetic hyperthermia and the versatility of HLPNPs to deliver different drugs to a selected target, it is possible to design a multiplatform where hyperthermia treatments and conventional chemotherapy are used in the same nano-system with increased efficacy.

4.1 Active targeting

In order to be effective and selective, this delivery system has to be localized as close as possible to the target tumoral cells. Functionalization of nanoparticles is typically applied for NPs employed in the biomedical field. With functionalization, one refers to the surface modification of NPs by the conjugation of proteins or other bio molecules on to the surface, to enhance the interaction with the target and identify it with high accuracy. In addition to targeting, functionalization improves physical properties and enhances the stability of NPs. Active targeting of lipidic structures is a quite diffused way to enhance interaction between cancer cells and nano-delivery platforms [3, 69, 70].
Folic acid conjugation, for example, results as an effective targeting strategy since various kinds of cancer exhibit the overexpression of the folate receptor. Liu et al. [71] found out that FA conjugation caused a slight increase of HLPNPs dimension ($\sim$ 260nm vs $\sim$ 200nm) and a slight decrease of the ζ-potential from $\sim$26 mV to $\sim$21 mV, but the encapsulation efficiency and the release profile remained almost the same. However, the uptake of the nanoparticles by the MCF7 breast cancer cells and NIH/3T3 fibroblast cells was enhanced by the functionalization. For instance, after 2 h of incubation, the cellular uptake of FA-functionalized HLPNPs resulted $\sim$60% higher than non-functionalized nanovectors (uptake efficiency of $\sim$40%). This effect resulted in enhanced cytotoxicity for the cells culture: data show that after 72 h of incubation with the drug-loaded FA-conjugated HLPNPs, the amount of surviving cells was $\sim$12% while the culture treated with non-targeted HLPNPs exhibited twofold living cells.
Similarly Agrawal et al. [72] showed increased T98G cells uptake for FA-functionalized vectors, with 97.7% uptake for folic acid (F) decorated polymer lipid hybrid nanoparticles (PLNs) encapsulating cyclo-[Arg-GlyAsp-D-Phe-Lys] (cRGDfK) modified paclitaxel (PtxR-FPLNs).

Apart from FA, other active targeting moieties can be conjugated to the lipid-PEG shell, demonstrating the high efficacy of active targeting.
Zhang et al. [15] used A10 RNA aptamer to target specific membrane proteins expressed in prostate cancer cells. Results demonstrated high uptake ratio from cells expressing this protein as compared to cells not expressing it. Messerschmidt et al. [18] as well, got similar results for HLPNPs encapsulating in the polymeric core the single chain tumor necrosis factor (scTNF) and having a shell functionalized with single chain variable fragments (ScFv) targeting the fibroblast activation protein (FAP). The lipidic shell prevented the expression of TNF against every tissue, before internalization; only once the nanovector was internalized by a cells, and therefore degraded, the TNF was able to trigger cell necrosis. Their data clearly showed that thanks to the surface targeting, nanovectors were easily uptaken by FAP-expressing HT1080 fibrosarcoma cells. On the contrary, HLPNPs were not internalized by FAP-negative cells. This suggested that the lipid coating of such carriers minimized the non-specific binding of the polystyrene core toward FAP-negative cells, reducing the scTNF-mediated cytotoxicity of healthy cells. Therefore, hybrid NPs were superior in terms of the specific non-targeting, hence safety for healthy cells.

4.2 Superparamagnetic iron-oxide nanoparticles loaded hybrid lipid/polymer nanoparticles

By simply modifying the synthesis techniques described in the previous chapters, it is possible to produce HLPNPs loaded with SPIONs . For both ESE and nanoprecipitation methods, the colloidal suspension of monodisperse SPIONs is conserved in the organic solvent (typically THF) where are also dissolved the polymer and dispersed the drug; thus during the self-assembly processes, the SPIONs will be entrapped inside the polymeric core along with the drug [2]. The heat generated by the loaded SPIONs , beside hyperthermia treatments, is exploited to trigger the drug release on demand. Indeed, HLPNPs showed reduced water permeabilization and thus a slower and not complete cargo unload with respect to polymeric-NPs used for the same application. This is due to the lipidic shell, that protects the inner core from water infiltration prolonging the structural integrity and reducing the drug leakage. Hence, by heating the vector from the inside by an external *stimulus*, it can be triggered the carrier degradation and thus the drug dispersion.
Kong et al. [2] synthesized 80 nm PLGA/soybean lecithin hybrid vectors loaded with 10 nm SPIONs and camptothecin (CPT) and demonstrated how the AMF stimulation triggers the drug release, improving the administration of CPT and enhancing the cytotoxic effect. This SPIONs loaded nanovectors subjected to a RF magnetic field reached 60% of drug release, after just 5 hours (100% after 45 h), whereas not stimulated by the same RF field or without SPIONs in their core, released just the 15% of the loaded drug after 45 h. As a further validation of the effectiveness of this multifunctional delivery vector, the same work showed a reduced growth rate of breast cancer cells when treated with SPIONs -lipid-PLGA hybrid nanoparticles loaded with CMT and stimulated with AMF.
Tan et al. [7] reported as well, enhanced cells cytotoxicity when combining both hyperthermia and chemotherapeutic agents, because of a permeabilization of the lysosomal membrane after SPIONs heat generation due to AMF stimulation.
Tapeinos et al. [12] as well conducted a similar experiment [2] employing temozolomide and SPIONs loaded lipid nanovectors (LMNVs). They demonstrated that U-87 MG cultures treated with TMZ-loaded LMNVs and stimulated with AMF underwent apoptosis, while without AMF excitation and simple TMZ lipid nanoparticles, only $\sim$12% of the cells underwent apoptosis.
The same group also reported these nanovectors ability to pass through an *in vitro* model of the

BBB. After 24 h, they measured that the 40% of the DiO-stained LMNVs overcame the BBB and thus could be internalized by glioblastoma tumoral cells.
Marino et al. [73] studied a similar system composed of TMZ-loaded LMNVs and interestingly investigated the possibility to enhance this barrier crossing by applying a static magnetic field (SMF). LMNVs functionalized with an antibody against transferrin receptor (AbLMNVs) showed a significant increase (7-fold) of BBB crossing when exposed to this SMF.
In vivo tests were also conducted by Dilnawaz et al. [53] reporting that paclitaxel loaded magnetic delivery vectors showed 50 μg/g tissue accumulation for *in vivo* brain tissues even 48 h after the administration while the free drug showed an accumulation of 18 μg/g tissue 30 minutes after the administration, which decreased to a non-detectable range in just six hours. These results clearly show how nano-drug delivery systems highly increase the cells retention of drugs, extending the exposure time and thus improving the cytotoxic efficacy.

Imaging functionality could be also integrated in the SPIONs loaded HLPNPs by exploiting the magnetic resonance of such superparamagnetic components.
In order to increase the contrast in MRI and enhance the resolution, Gd^{3+} based contrast agents are the gold standard contrast medium on the market. These compounds allows a good quality MRI, but they have to be finely dosed since, recently, they have been linked to toxic effect towards kidneys and liver.
In this field, SPIONs showed as a more sensitive contrast medium; the obtained images have better resolution, and the particles have a better retention time *in vivo* and are more biocompatible.
Thus, HLPNPs carrying SPIONs and drug, would combine the therapeutic properties with the imaging ability, creating a precise and effective theranostic device [54, 74, 75].

Conclusions

This class of multifunctional delivery platforms promises to solve, or at least reduce, drawbacks linked to specific treatments.
HLPNPs allow a wide choice among several types of structural components according to the property of the chosen drug. Several possibilities have been exploited, allowing administration of therapeutics aimed at different kind of tumors, from brain GBM to prostate cancer. Soon mass scale production systems will be available allowing possible clinical trials; thanks to the improvement of synthesis procedures, high reproducibility and good tuning of NPs properties, are guaranteed high biocompatibility and minimal adverse effects.
Surface targeting along with magnetic delivery permit the penetration of physiological barriers, along with a high concentration of the therapeutics to the target site, avoiding the diffusion of possible toxic substances to healthy tissues. Multidrug resistance due to poor drug distribution could be overcame by combining different therapeutic approaches at the same time.
Furthermore, thanks to the magnetic properties of SPIONs, it is possible to exploit possible MRI application, upgrading from therapeutic device to theranostic device.

Bibliography

[1] Ahmedin Jemal Lindsey Torre Isabelle Soerjomataram Freddie Bray and Cary Adams. *Third Edition THE CANCER ATLAS Third Edition THE CANCER ATLAS 4 5*. ISBN: 978-1-60443-265-7. URL: www.cancer.org (cit. on p. ii).

[2] Seong Deok Kong, Marta Sartor, Che Ming Jack Hu, Weizhou Zhang, Liangfang Zhang, and Sungho Jin. «Magnetic field activated lipid-polymer hybrid nanoparticles for stimuli-responsive drug release». In: *Acta Biomaterialia* 9 (3 Mar. 2013), pp. 5447–5452. ISSN: 17427061. DOI: 10.1016/j.actbio.2012.11.006 (cit. on pp. iii, 10, 17).

[3] Kunn Hadinoto, Ajitha Sundaresan, and Wean Sin Cheow. «Lipid-polymer hybrid nanoparticles as a new generation therapeutic delivery platform: A review». In: *European Journal of Pharmaceutics and Biopharmaceutics* 85 (3 PART A 2013), pp. 427–443. ISSN: 18733441. DOI: 10.1016/j.ejpb.2013.07.002 (cit. on pp. iii, 3, 7, 16).

[4] Tushar Date, Vaishnavi Nimbalkar, Jyostna Kamat, Anupama Mittal, Ram I. Mahato, and Deepak Chitkara. «Lipid-polymer hybrid nanocarriers for delivering cancer therapeutics». In: *Journal of Controlled Release* 271 (Feb. 2018), pp. 60–73. ISSN: 18734995. DOI: 10.1016/j.jconrel.2017.12.016 (cit. on p. iii).

[5] Maribella Domenech, Ileana Marrero-Berrios, Madeline Torres-Lugo, and Carlos Rinaldi. «Lysosomal membrane permeabilization by targeted magnetic nanoparticles in alternating magnetic fields». In: *ACS Nano* 7 (6 June 2013), pp. 5091–5101. ISSN: 19360851. DOI: 10.1021/nn4007048 (cit. on p. iii).

[6] Claire Sanchez et al. «Targeting a G-protein-coupled receptor overexpressed in endocrine tumors by magnetic nanoparticles to induce cell death». In: *ACS Nano* 8 (2 Feb. 2014), pp. 1350–1363. ISSN: 19360851. DOI: 10.1021/nn404954s (cit. on p. iii).

[7] R. P. Tan, J. Carrey, and M. Respaud. «Magnetic hyperthermia properties of nanoparticles inside lysosomes using kinetic Monte Carlo simulations: Influence of key parameters and dipolar interactions, and evidence for strong spatial variation of heating power». In: *Physical Review B - Condensed Matter and Materials Physics* 90 (21 Dec. 2014). ISSN: 1550235X. DOI: 10.1103/PhysRevB.90.214421 (cit. on pp. iii, 17).

[8] Jayanta Kumar Patra et al. «Nano based drug delivery systems: Recent developments and future prospects 10 Technology 1007 Nanotechnology 03 Chemical Sciences 0306 Physical Chemistry (incl. Structural) 03 Chemical Sciences 0303 Macromolecular and Materials Chemistry 11 Medical and Health Sciences 1115 Pharmacology and Pharmaceutical Sciences 09 Engineering 0903 Biomedical Engineering Prof Ueli Aebi, Prof Peter Gehr». In: *Journal of Nanobiotechnology* 16 (1 Sept. 2018). ISSN: 14773155. DOI: 10.1186/s12951-018-0392-8 (cit. on p. 2).

[9] Rebecca L. McCall and Rachael W. Sirianni. «PLGA nanoparticles formed by single- or double-emulsion with vitamin E-TPGS.» In: *Journal of visualized experiments : JoVE* (82 2013), p. 51015. ISSN: 1940087X. DOI: 10.3791/51015 (cit. on p. 2).

[10] Yichao Wang, Puwang Li, Thao Truong Dinh Tran, Juan Zhang, and Lingxue Kong. «Manufacturing techniques and surface engineering of polymer based nanoparticles for targeted drug delivery to cancer». In: *Nanomaterials* 6 (2 Feb. 2016). ISSN: 20794991. DOI: 10.3390/nano6020026 (cit. on pp. 2, 4–7).

[11] Tivadar Feczkó, Albrecht Piiper, Thomas Pleli, Christian Schmithals, Dominic Denk, Stephanie Hehlgans, Franz Rödel, Thomas J. Vogl, and Matthias G. Wacker. «Theranostic sorafenib-loaded polymeric nanocarriers manufactured by enhanced gadolinium conjugation techniques». In: *Pharmaceutics* 11 (10 Oct. 2019). ISSN: 19994923. DOI: 10.3390/pharmaceutics11100489 (cit. on p. 2).

[12] Christos Tapeinos et al. «Stimuli-responsive lipid-based magnetic nanovectors increase apoptosis in glioblastoma cells through synergic intracellular hyperthermia and chemotherapy». In: *Nanoscale* 11 (1 Jan. 2019), pp. 72–88. ISSN: 20403372. DOI: 10.1039/c8nr05520c (cit. on pp. 3, 17).

[13] Danilo D. Lasic. «Doxorubicin in sterically stabilized liposomes». In: *Nature* 380 (Apr. 1996), pp. 561–562. DOI: doi:10.1038/380561a0. URL: https://doi.org/10.1038/380561a0 (cit. on p. 3).

[14] I Judson et al. *Randomised phase II trial of pegylated liposomal doxorubicin (DOXIL 1 /CAELYX 1) versus doxorubicin in the treatment of advanced or metastatic soft tissue sarcoma: a study by the EORTC Soft Tissue and Bone Sarcoma Group*. 2001, pp. 870–877. URL: www.ejconline.com (cit. on p. 3).

[15] Liangfang Zhang, Juliana M. Chan, Frank X. Gu, June Wha Rhee, Andrew Z. Wang, Aleksandar F. Radovic-Moreno, Frank Alexis, Robert Langer, and Omid C. Farokhzad. «Self-assembled lipid-polymer hybrid nanoparticles: A robust drug delivery platform». In: *ACS Nano* 2 (8 Aug. 2008), pp. 1696–1702. ISSN: 19360851. DOI: 10.1021/nn800275r (cit. on pp. 3, 5–8, 17).

[16] Che-Ming J Hu, Li Zhang, Santosh Aryal, Connie Cheung, Ronnie H Fang, and Liangfang Zhang. «Erythrocyte membrane-camouflaged polymeric nanoparticles as a biomimetic delivery platform». In: *Source* 108 (27 2011), pp. 10980–10985. DOI: 10.1073/pnas. URL: http://www.jstor.orgURL:http://www.jstor.org/stable/27978728 (cit. on p. 3).

[17] Xiaoyang Xu et al. «Enhancing tumor cell response to chemotherapy through nanoparticle-mediated codelivery of siRNA and cisplatin prodrug». In: *Proceedings of the National Academy of Sciences of the United States of America* 110 (46 Nov. 2013), pp. 18638–18643. ISSN: 00278424. DOI: 10.1073/pnas.1303958110 (cit. on pp. 4, 5, 7).

[18] Sylvia K.E. Messerschmidt, Anna Musyanovych, Martin Altvater, Peter Scheurich, Klaus Pfizenmaier, Katharina Landfester, and Roland E. Kontermann. «Targeted lipid-coated nanoparticles: Delivery of tumor necrosis factor-functionalized particles to tumor cells». In: *Journal of Controlled Release* 137 (1 July 2009), pp. 69–77. ISSN: 01683659. DOI: 10.1016/j.jconrel.2009.03.010 (cit. on pp. 4, 17).

[19] Cory J. Hitzman, William F. Elmquist, Lee W. Wattenberg, and Timothy S. Wiedmann. «Development of a respirable, sustained release microcarrier for 5-fluorouracil I: In vitro assessment of liposomes, microspheres, and lipid coated nanoparticles». In: *Journal of Pharmaceutical Sciences* 95 (5 2006), pp. 1114–1126. ISSN: 15206017. DOI: 10.1002/jps.20591 (cit. on p. 4).

[20] Warefta Hasan et al. «Delivery of multiple siRNAs using lipid-coated PLGA nanoparticles for treatment of prostate cancer». In: *Nano Letters* 12 (1 Jan. 2012), pp. 287–292. ISSN: 15306984. DOI: 10.1021/nl2035354 (cit. on p. 4).

[21] Ronnie H. Fang, Santosh Aryal, Che Ming Jack Hu, and Liangfang Zhang. «Quick synthesis of lipid-polymer hybrid nanoparticles with low polydispersity using a single-step sonication method». In: *Langmuir* 26 (22 Nov. 2010), pp. 16958–16962. ISSN: 07437463. DOI: 10.1021/la103576a (cit. on pp. 4, 6, 7).

[22] Emilia Pisani, Elias Fattal, Juliane Paris, Catherine Ringard, Véronique Rosilio, and Nicolas Tsapis. «Surfactant dependent morphology of polymeric capsules of perfluorooctyl bromide: Influence of polymer adsorption at the dichloromethane-water interface». In: *Journal of Colloid and Interface Science* 326 (1 Oct. 2008), pp. 66–71. ISSN: 00219797. DOI: 10.1016/j.jcis.2008.07.013 (cit. on p. 4).

[23] S. Hariharan, V. Bhardwaj, I. Bala, J. Sitterberg, U. Bakowsky, and M. N.V. Ravi Kumar. «Design of estradiol loaded PLGA nanoparticulate formulations: A potential oral delivery system for hormone therapy». In: *Pharmaceutical Research* 23 (1 Jan. 2006), pp. 184–195. ISSN: 07248741. DOI: 10.1007/s11095-005-8418-y (cit. on pp. 4, 7).

[24] Bivash Mandal, Himanshu Bhattacharjee, Nivesh Mittal, Hongkee Sah, Pavan Balabathula, Laura A. Thoma, and George C. Wood. «Core-shell-type lipid-polymer hybrid nanoparticles as a drug delivery platform». In: *Nanomedicine: Nanotechnology, Biology, and Medicine* 9 (4 May 2013), pp. 474–491. ISSN: 15499634. DOI: 10.1016/j.nano.2012.11.010 (cit. on pp. 5–7).

[25] Khin Yin Win and Si Shen Feng. «Effects of particle size and surface coating on cellular uptake of polymeric nanoparticles for oral delivery of anticancer drugs». In: *Biomaterials* 26 (15 May 2005), pp. 2713–2722. ISSN: 01429612. DOI: 10.1016/j.biomaterials.2004.07.050 (cit. on pp. 5, 7).

[26] Wean Sin Cheow and Kunn Hadinoto. «Factors affecting drug encapsulation and stability of lipid-polymer hybrid nanoparticles». In: *Colloids and Surfaces B: Biointerfaces* 85 (2 July 2011), pp. 214–220. ISSN: 09277765. DOI: 10.1016/j.colsurfb.2011.02.033 (cit. on pp. 5, 7).

[27] Yutao Liu, Jie Pan, and Si Shen Feng. «Nanoparticles of lipid monolayer shell and biodegradable polymer core for controlled release of paclitaxel: Effects of surfactants on particles size, characteristics and in vitro performance». In: *International Journal of Pharmaceutics* 395 (1-2 Aug. 2010), pp. 243–250. ISSN: 03785173. DOI: 10.1016/j.ijpharm.2010.05.008 (cit. on pp. 5, 7).

[28] Chih Hang Chu, Yu Chao Wang, Hsin Ying Huang, Li Chen Wu, and Chung Shi Yang. «Ultrafine PEG-coated poly(lactic-co-glycolic acid) nanoparticles formulated by hydrophobic surfactant-assisted one-pot synthesis for biomedical applications». In: *Nanotechnology* 22 (18 May 2011). ISSN: 09574484. DOI: 10.1088/0957-4484/22/18/185601 (cit. on pp. 5, 7).

[29] Jinjun Shi, Zeyu Xiao, Alexander R. Votruba, Cristian Vilos, and Omid C. Farokhzad. «Differentially charged hollow core/shell lipid-polymer-lipid hybrid nanoparticles for small interfering rna delivery». In: *Angewandte Chemie - International Edition* 50 (31 July 2011), pp. 7027–7031. ISSN: 14337851. DOI: 10.1002/anie.201101554 (cit. on pp. 5, 7).

[30] H Fessi, F Puisieux, J Ph Devissaguet, N Ammoury, and S Benita. *Rapid Communication Nanocapsule formation by interfacial polymer deposition following solvent displacement.* 1989, p. 55 (cit. on p. 5).

[31] Carlos Gregorio Barreras-Urbina, Benjamín Ramírez-Wong, Guadalupe Amanda López-Ahumada, Silvia Elena Burruel-Ibarra, Oliviert Martínez-Cruz, José Agustín Tapia-Hernández, and Francisco Rodríguez Félix. «Nano- and Micro-Particles by Nanoprecipitation: Possible Application in the Food and Agricultural Industries». In: *International Journal of Food Properties* 19 (9 Sept. 2016), pp. 1912–1923. ISSN: 15322386. DOI: 10.1080/10942912.2015.1089279 (cit. on p. 6).

[32] J. G.J.L. Lebouille, R. Stepanyan, J. J.M. Slot, M. A. Cohen Stuart, and R. Tuinier. «Nanoprecipitation of polymers in a bad solvent». In: *Colloids and Surfaces A: Physicochemical and Engineering Aspects* 460 (Dec. 2013), pp. 225–235. ISSN: 18734359. DOI: 10.1016/j.colsurfa.2013.11.045 (cit. on p. 6).

[33] Juliana M. Chan, Liangfang Zhang, Kai P. Yuet, Grace Liao, June Wha Rhee, Robert Langer, and Omid C. Farokhzad. «PLGA-lecithin-PEG core-shell nanoparticles for controlled drug delivery». In: *Biomaterials* 30 (8 Mar. 2009), pp. 1627–1634. ISSN: 01429612. DOI: 10.1016/j.biomaterials.2008.12.013 (cit. on pp. 6, 7).

[34] Xian Zhu Yang, Shuang Dou, Yu Cai Wang, Hong Yan Long, Meng Hua Xiong, Cheng Qiong Mao, Yan Dan Yao, and Jun Wang. «Single-step assembly of cationic lipid-polymer hybrid nanoparticles for systemic delivery of siRNA». In: *ACS Nano* 6 (6 June 2012), pp. 4955–4965. ISSN: 19360851. DOI: 10.1021/nn300500u (cit. on pp. 6, 7).

[35] Pedro M. Valencia, Pamela A. Basto, Liangfang Zhang, Minsoung Rhee, Robert Langer, Omid C. Farokhzad, and Rohit Karnik. «Single-step assembly of homogenous lipid-polymeric and lipid-quantum dot nanoparticles enabled by microfluidic rapid mixing». In: *ACS Nano* 4 (3 Mar. 2010), pp. 1671–1679. ISSN: 19360851. DOI: 10.1021/nn901433u (cit. on p. 7).

[36] Yongtae Kim, Bomy Lee Chung, Mingming Ma, Willem J.M. Mulder, Zahi A. Fayad, Omid C. Farokhzad, and Robert Langer. «Mass production and size control of lipid-polymer hybrid nanoparticles through controlled microvortices». In: *Nano Letters* 12 (7 July 2012), pp. 3587–3591. ISSN: 15306992. DOI: 10.1021/nl301253v (cit. on p. 7).

[37] Rajendran J.C. Bose, Rramaswamy Ravikumar, Vengadeshprabu Karuppagounder, Devasier Bennet, Sabarinathan Rangasamy, and Rajarajan A. Thandavarayan. «Lipid–polymer hybrid nanoparticle-mediated therapeutics delivery: advances and challenges». In: *Drug Discovery Today* 22 (8 Aug. 2017), pp. 1258–1265. ISSN: 18785832. DOI: 10.1016/j.drudis.2017.05.015 (cit. on p. 7).

[38] Chiara Martinelli, Carlotta Pucci, and Gianni Ciofani. «Nanostructured carriers as innovative tools for cancer diagnosis and therapy». In: *APL Bioengineering* 3 (1 Mar. 2019), p. 011502. ISSN: 2473-2877. DOI: 10.1063/1.5079943 (cit. on p. 7).

[39] Yu Zheng et al. «Transferrin-conjugated lipid-coated PLGA nanoparticles for targeted delivery of aromatase inhibitor 7-APTADD to breast cancer cells». In: *International Journal of Pharmaceutics* 390 (2 May 2010), pp. 234–241. ISSN: 03785173. DOI: 10.1016/j.ijpharm.2010.02.008 (cit. on p. 7).

[40] Jens Overgaard. *EFFECT OF HYPERTHERMIA O N MALIGNANT CELLS IN VIVO A Review and a Hypothesis*. 1977, pp. 2637–2646 (cit. on p. 9).

[41] Keon Mahmoudi, Alexandros Bouras, Dominique Bozec, Robert Ivkov, and Constantinos Hadjipanayis. «Magnetic hyperthermia therapy for the treatment of glioblastoma: a review of the therapy's history, efficacy and application in humans». In: *International Journal of Hyperthermia* 34 (8 Nov. 2018), pp. 1316–1328. ISSN: 14645157. DOI: 10.1080/02656736.2018.1430867 (cit. on p. 9).

[42] Rolf D. Issels. «Hyperthermia adds to chemotherapy». In: *European Journal of Cancer* 44 (17 Nov. 2008), pp. 2546–2554. ISSN: 09598049. DOI: 10.1016/j.ejca.2008.07.038 (cit. on p. 9).

[43] George M Hahn. *Potential for Therapy of Drugs and Hyperthermia'*. 1979, pp. 2264–2268 (cit. on p. 9).

[44] Margarethus M. Paulides, Paul R. Stauffer, Esra Neufeld, Paolo F. MacCarini, Adamos Kyriakou, Richard A.M. Canters, Chris J. Diederich, Jurriaan F. Bakker, and Gerard C. Van Rhoon. «Simulation techniques in hyperthermia treatment planning». In: *International Journal of Hyperthermia* 29 (4 2013), pp. 346–357. ISSN: 14645157. DOI: 10.3109/02656736.2013.790092 (cit. on p. 9).

[45] P. Wust, B. Hildebrandt, G. Sreenivasa, B. Rau, J. Gellermann, H. Riess, R. Felix, and Pm Schlag. «Hyperthermia in combined treatment of cancer». In: *Lancet Oncology* 3 (8 2002), pp. 487–497. ISSN: 14702045. DOI: 10.1016/S1470-2045(02)00818-5 (cit. on p. 9).

[46] Jianan Wang. *Simulation of Magnetic Nanoparticle Hyperthermia in Prostate Tumors*. 2014 (cit. on p. 9).

[47] Cindi L. Dennis and Robert Ivkov. «Physics of heat generation using magnetic nanoparticles for hyperthermia». In: *International Journal of Hyperthermia* 29 (8 2013), pp. 715–729. ISSN: 14645157. DOI: 10.3109/02656736.2013.836758 (cit. on pp. 9, 11–14).

[48] Qing Li, Christina W. Kartikowati, Shinji Horie, Takashi Ogi, Toru Iwaki, and Kikuo Okuyama. «Correlation between particle size/domain structure and magnetic properties of highly crystalline Fe3O4 nanoparticles». In: *Scientific Reports* 7 (1 Dec. 2017). ISSN: 20452322. DOI: 10.1038/s41598-017-09897-5 (cit. on pp. 10, 11).

[49] Minhong Jeun, Yu Jeong Kim, Ki Ho Park, Sun Ha Paek, and Seongtae Bae. «Physical contribution of néel and brown relaxation to interpreting intracellular hyperthermia characteristics using superparamagnetic nanofluids». In: *Journal of Nanoscience and Nanotechnology* 13 (8 Aug. 2013), pp. 5719–5725. ISSN: 15334880. DOI: 10.1166/jnn.2013.7524 (cit. on pp. 10, 12, 14).

[50] Tristan D. Clemons, Roland H. Kerr, and Alexander Joos. *Multifunctional magnetic nanoparticles: Design, synthesis, and biomedical applications*. Jan. 2019. DOI: 10.1016/B978-0-12-803581-8.10462-X (cit. on pp. 10, 11, 13).

[51] Carlos Martinez-Boubeta et al. «Learning from nature to improve the heat generation of iron-oxide nanoparticles for magnetic hyperthermia applications». In: *Scientific Reports* 3 (Apr. 2013). ISSN: 20452322. DOI: 10.1038/srep01652 (cit. on pp. 10, 11).

[52] Boubker Mehdaoui, Anca Meffre, Julian Carrey, Sébastien Lachaize, Lise Marie Lacroix, Michel Gougeon, Bruno Chaudret, and Marc Respaud. «Optimal size of nanoparticles for magnetic hyperthermia: A combined theoretical and experimental study». In: *Advanced Functional Materials* 21 (23 Dec. 2011), pp. 4573–4581. ISSN: 1616301X. DOI: 10.1002/adfm.201101243 (cit. on p. 10).

[53] Fahima Dilnawaz, Abhalaxmi Singh, Sujeet Mewar, Uma Sharma, N. R. Jagannathan, and Sanjeeb Kumar Sahoo. «The transport of non-surfactant based paclitaxel loaded magnetic nanoparticles across the blood brain barrier in a rat model». In: *Biomaterials* 33 (10 Apr. 2012), pp. 2936–2951. ISSN: 01429612. DOI: 10.1016/j.biomaterials.2011.12.046 (cit. on pp. 10, 18).

[54] Selim Sulek, Busra Mammadov, Davut I. Mahcicek, Huseyin Sozeri, Ergin Atalar, Ayse B. Tekinay, and Mustafa O. Guler. «Peptide functionalized superparamagnetic iron oxide nanoparticles as MRI contrast agents». In: *Journal of Materials Chemistry* 21 (39 Oct. 2011), pp. 15157–15162. ISSN: 09599428. DOI: 10.1039/c1jm11387a (cit. on pp. 10, 18).

[55] C L Dennis et al. *The defining length scales of mesomagnetism: a review*. 2002, pp. 1175–1262. URL: http://iopscience.iop.org/0953-8984/14/49/201 (cit. on pp. 11, 13).

[56] Silvio Dutz and Rudolf Hergt. «Magnetic nanoparticle heating and heat transfer on a microscale: Basic principles, realities and physical limitations of hyperthermia for tumour therapy». In: *International Journal of Hyperthermia* 29 (8 2013), pp. 790–800. ISSN: 14645157. DOI: 10.3109/02656736.2013.822993 (cit. on pp. 11–13).

[57] R E Rosensweig. *Heating magnetic fluid with alternating magnetic field*. 2002, pp. 370–374 (cit. on pp. 11–14).

[58] Aziliz Hervault and Nguyen Thi Kim Thanh. «Magnetic nanoparticle-based therapeutic agents for thermo-chemotherapy treatment of cancer». In: *Nanoscale* 6 (20 Oct. 2014), pp. 11553–11573. ISSN: 20403372. DOI: 10.1039/c4nr03482a (cit. on pp. 11, 13).

[59] B. B. Lahiri, Surojit Ranoo, and John Philip. «Uncertainties in the estimation of specific absorption rate during radiofrequency alternating magnetic field induced non-adiabatic heating of ferrofluids». In: *Journal of Physics D: Applied Physics* 50 (45 Oct. 2017). ISSN: 13616463. DOI: 10.1088/1361-6463/aa89de (cit. on pp. 11, 13).

[60] Alison E. Deatsch and Benjamin A. Evans. «Heating efficiency in magnetic nanoparticle hyperthermia». In: *Journal of Magnetism and Magnetic Materials* 354 (2014), pp. 163–172. ISSN: 03048853. DOI: 10.1016/j.jmmm.2013.11.006 (cit. on pp. 11, 13, 14).

[61] Rudolf Hergt and Silvio Dutz. «Magnetic particle hyperthermia-biophysical limitations of a visionary tumour therapy». In: *Journal of Magnetism and Magnetic Materials* 311 (1 SPEC. ISS. 2007), pp. 187–192. ISSN: 03048853. DOI: 10.1016/j.jmmm.2006.10.1156 (cit. on pp. 12, 14).

[62] Suriyanto, E. Y.K. Ng, and S. D. Kumar. «Physical mechanism and modeling of heat generation and transfer in magnetic fluid hyperthermia through Néelian and Brownian relaxation: a review». In: *Biomedical engineering online* 16 (1 Mar. 2017), p. 36. ISSN: 1475925X. DOI: 10.1186/s12938-017-0327-x (cit. on pp. 12–14).

[63] R. R. Wildeboer, P. Southern, and Q. A. Pankhurst. «On the reliable measurement of specific absorption rates and intrinsic loss parameters in magnetic hyperthermia materials». In: *Journal of Physics D: Applied Physics* 47 (49 Dec. 2014). ISSN: 13616463. DOI: 10.1088/0022-3727/47/49/495003 (cit. on p. 12).

[64] Vanchna Singh, Varsha Banerjee, and Manish Sharma. «Dynamics of magnetic nanoparticle suspensions». In: (Aug. 2012). URL: http://arxiv.org/abs/1208.4061 (cit. on pp. 12–14).

[65] J. M.D. Coey. «Louis Néel: Retrospective (invited)». In: vol. 93. May 2003, pp. 8224–8229. DOI: 10.1063/1.1557815 (cit. on p. 13).

[66] Azhar Zahoor Abbasi et al. «Magnetic capsules for NMR imaging: Effect of magnetic nanoparticles spatial distribution and aggregation». In: *Journal of Physical Chemistry C* 115 (14 Apr. 2011), pp. 6257–6264. ISSN: 19327447. DOI: 10.1021/jp1118234 (cit. on p. 14).

[67] Bochu Wang, Yang Cao, Lichun Yang, and Yazhou Wang. «Rheological properties of PLGA-PEG-PLGA copolymers for ophthalmic injection». In: *Journal of Applied Polymer Science* 125 (1 July 2012), pp. 370–375. ISSN: 00218995. DOI: 10.1002/app.35584 (cit. on p. 14).

[68] Lorena Maldonado-Camargo, Mythreyi Unni, and Carlos Rinaldi. *Magnetic characterization of iron oxide nanoparticles for biomedical applications*. 2017. DOI: 10.1007/978-1-4939-6840-4_4 (cit. on p. 14).

[69] Sumith A. Kularatne and Philip S. Low. «Targeting of nanoparticles: folate receptor.» In: *Methods in molecular biology (Clifton, N.J.)* 624 (2010), pp. 249–265. ISSN: 19406029. DOI: 10.1007/978-1-60761-609-2_17 (cit. on p. 16).

[70] Rukmani Thiruppathi, Sachin Mishra, Mathangi Ganapathy, Parasuraman Padmanabhan, and Balázs Gulyás. «Nanoparticle functionalization and its potentials for molecular imaging». In: *Advanced Science* 4 (3 Mar. 2017). ISSN: 21983844. DOI: 10.1002/advs.201600279 (cit. on p. 16).

[71] Yutao Liu, Kai Li, Jie Pan, Bin Liu, and Si Shen Feng. «Folic acid conjugated nanoparticles of mixed lipid monolayer shell and biodegradable polymer core for targeted delivery of Docetaxel». In: *Biomaterials* 31 (2 Jan. 2010), pp. 330–338. ISSN: 01429612. DOI: 10.1016/j.biomaterials.2009.09.036 (cit. on p. 16).

[72] Udita Agrawal, Gousia Chashoo, Parduman Raj Sharma, Ashok Kumar, Ajit Kumar Saxena, and S. P. Vyas. «Tailored polymer-lipid hybrid nanoparticles for the delivery of drug conjugate: Dual strategy for brain targeting». In: *Colloids and Surfaces B: Biointerfaces* 126 (Feb. 2015), pp. 414–425. ISSN: 18734367. DOI: 10.1016/j.colsurfb.2014.12.045 (cit. on p. 16).

[73] Attilio Marino et al. «Multifunctional temozolomide-loaded lipid superparamagnetic nanovectors: Dual targeting and disintegration of glioblastoma spheroids by synergic chemotherapy and hyperthermia treatment». In: *Nanoscale* 11 (44 Nov. 2019), pp. 21227–21248. ISSN: 20403372. DOI: 10.1039/c9nr07976a (cit. on p. 18).

[74] Yuan Qiu, Raghavendra Palankar, María Echeverría, Nikolay Medvedev, Sergio E. Moya, and Mihaela Delcea. «Design of hybrid multimodal poly(lactic-co-glycolic acid) polymer nanoparticles for neutrophil labeling, imaging and tracking». In: *Nanoscale* 5 (24 2013), pp. 12624–12632. ISSN: 20403364. DOI: 10.1039/c3nr04013e (cit. on p. 18).

[75] Paula Solar, Guillermo González, Cristian Vilos, Natalia Herrera, Natalia Juica, Mabel Moreno, Felipe Simon, and Luis Velásquez. «Multifunctional polymeric nanoparticles doubly loaded with SPION and ceftiofur retain their physical and biological properties». In: *Journal of Nanobiotechnology* 13 (1 Feb. 2015). ISSN: 14773155. DOI: 10.1186/s12951-015-0077-5 (cit. on p. 18).